

Research Paper

## Multiwalled Carbon Nanotubes Interact with Macrophages and Influence Tumor Progression and Metastasis

Man Yang<sup>\*1,2</sup>, Jie Meng<sup>\*1</sup>, Xuelian Cheng<sup>1</sup>, Jing Lei<sup>1</sup>, Hua Guo<sup>1</sup>, Weiqi Zhang<sup>1</sup>, Hua Kong<sup>1</sup>, Haiyan Xu<sup>1</sup> 

1. Department of Biomedical Engineering, Institute of Basic Medical Sciences, Chinese Academy of Medical Sciences and Peking Union Medical College, Beijing 100005, P. R. China.

2. School of Public Health and Family Medicine, Capital Medical University, Beijing 100069, P. R. China.

\* These authors contributed equally to this work.

 Corresponding author: xuhy@pumc.edu.cn.

© Ivyspring International Publisher. This is an open-access article distributed under the terms of the Creative Commons License (<http://creativecommons.org/licenses/by-nc-nd/3.0/>). Reproduction is permitted for personal, noncommercial use, provided that the article is in whole, unmodified, and properly cited.

Received: 2011.10.11; Accepted: 2011.12.06; Published: 2012.03.02

### Abstract

Macrophages are one of the most important types of immune effector cells and are closely associated with tumor progression and metastasis. In this work, we investigated the influences of oxidized multiwalled carbon nanotubes (o-MWCNT) on macrophages that are resting in the normal subcutis tissue or in the tumor microenvironment *in vivo* as well as on the macrophage cell line of RAW 264.7 treated with combination of IL4, IL10 and IL13 *in vitro*. The o-MWCNT were characterized with SEM, DLS, FTIR, TGA, and UV-vis-NIR spectroscopy, and their effects on the RAW 264.7 cell line and breast cancer tumor-bearing mice were analyzed using the MTS assay, flow cytometry analysis, and histological and immunohistochemical observations. Our experimental results showed that subcutaneously injected o-MWCNT not only induced phagocytosis of the local resident macrophages, but also competitively recruited macrophages from other tissues. These interactions resulted in macrophage reduction and decreased vessel density around the tumor mass, which together inhibited tumor progression and metastasis in the lung. In the cell line model, the o-MWCNT inhibited the ability of the interleukin treated RAW macrophages to promote tumor cell migration as well as decreased their proliferation rate.

Key words: MWCNT, macrophages, metastasis

### Introduction

In the tissue, macrophages differentiate from circulating monocytes and are one of the most types of important immune effector cells. They carry out a variety of functions, such as clearing cellular debris, responding to pathogens, and facilitating wound healing. In recent years, macrophages have been reported to take on different phenotypes and play different roles depending on the environmental signals that they receive. When circulating monocytes differentiate in a Th1 immune environment, the resulting

macrophages develop a classical M1 activation state; in contrast, when monocytes differentiate in a Th2 immune environment, the alternate M2 activation state is derived. In general, M1 macrophages promote antitumor responses by activating the adaptive immune system, while M2 macrophages enhance tumor growth by producing angiogenic factors, stromal breakdown factors, and downregulating antitumor immune responses [1]. On the spectrum of *in vivo* macrophage phenotypes, M1 and M2 likely represent

the two extremes and have different functions. In another recent review of the full spectrum of macrophage activation, it was suggested that macrophages should be classified into three major populations, including classically activated macrophages, wound-healing macrophages, and regulatory macrophages, because the M2 group has rapidly expanded to include essentially all macrophages that are not classically activated [2].

Aggressive or metastatic tumor cells can produce attractants to draw macrophages into the tumor microenvironment and then educate them to promote tumor progression [3]. These tumor-associated macrophages (TAMs) are in the alternate M2 activation state and exhibit characteristics of both wound-healing macrophages and regulatory macrophages, and produce cytokines and growth factors that can help tumor growth. Extensive research has demonstrated that macrophages in the tumor microenvironment are closely associated with the development and progression of a variety of tumors, such as breast cancer [4-5], prostate [6], glioma [7], lymphoma [8], bladder [9], lung [10], cervical [11] and melanoma [12]. TAMs have been investigated as a possible target for treating cancer. For example, Luo et al. has used RNAi technology to target legumain, a member of the asparaginyl endopeptidase family that functions as a stress protein and is overexpressed by TAM. Their experimental results demonstrated that a decrease of the number of TAMs in the tumor stroma effectively altered the tumor microenvironment to reduce tumor angiogenesis and progression, and thus markedly suppressed tumor growth and metastasis [13].

Carbon nanotubes based materials have shown promising potential in the biomedical field. Their possible use in novel delivery systems for drugs or DNA/RNA has been reviewed in detail by several recent publications [14-20]. We have previously reported that subcutaneously injected multiwalled carbon nanotubes in normal BALB/c mice were largely engulfed by resident macrophages around the injection site, inducing complement activation and short-term upregulation of some kinds of inflammatory cytokines in BALB/c mice [21]; and in tumor-bearing BALB/c mice subcutaneous injection of multiwalled carbon nanotubes inhibited the tumor progression to some extent [22]. When the multiwalled carbon nanotubes were used as a carrier of tumor lysate, subcutaneous injection of this conjugate in tumor-bearing mice effectively increased cytotoxicity of the lymphocytes to the tumor cells [23]. These findings imply that the inhibitory effect of multiwalled carbon nanotubes on tumor progression may

be associated with their interactions with macrophages. The aims of the present work are to investigate the influence of multiwalled carbon nanotubes on macrophages in the alternative activation state *in vitro* and in the tumor-bearing mice *in vivo*, and to explore whether these interactions can modify the tumor progression.

## Materials and Methods

**Preparation and Characterization of Oxidized Multi-walled Carbon Nanotubes:** Multi-walled carbon nanotubes (a-MWCNT; Chengdu Organic Chemicals Co. Ltd.) were prepared and characterized as previously described [24]. In brief, a-MWCNT was oxidized in concentrated H<sub>2</sub>SO<sub>4</sub>/HNO<sub>3</sub> (3:1 by volume) with sonication, followed by filtrating and washing with large amount of pure water to neutralize. The resulting oxidized MWCNT (o-MWCNT) was dispersed in water at different concentrations. The o-MWCNT solution was deposited by the drop-dry technique for characterization by X-ray photoelectron spectroscopy (XPS; Japan JEOL Scientific JPS-9010TR), Fourier transform infrared spectroscopy (FT-IR; Nicolet NEXUS 670), scanning electron microscopy (SEM; Hitachi S-5200), and thermogravimetric analysis (TGA; TG209C, NETZSCH). The solution of o-MWCNT was also analyzed by UV-Vis-NIR spectroscopy (Lambda 950, Perkin-Elmer) and dynamic light scattering spectroscopy (DLS ZEN 3690; Malvern Instruments Ltd, Malvern, UK).

**Cell Culture:** The mouse macrophage cell line RAW264.7 and mouse breast cancer cell line 4T1 were purchased from the Cell Bank of Shanghai Institutes of Biological Sciences, Chinese Academy of Sciences (Shanghai, China). RAW264.7 macrophages were maintained in RPMI1640 media supplemented with 10% fetal calf serum, 4 mM L-glutamine, 4500 mg/L glucose, 1500 mg/L sodium bicarbonate, and 0.1% each penicillin G and streptomycin (Invitrogen) at 37°C with 5% CO<sub>2</sub>. The 4T1 cell line is 6-thioguanine-resistant and derived from a BALB/c spontaneous mammary carcinoma; it was cultivated in RPMI1640 supplemented with 10% fetal calf serum, 2 mM L-glutamine, 4.5 g/L glucose, 1.5 g/L sodium bicarbonate, 10 mM HEPES, 1.0 mM sodium pyruvate, and 0.1% each penicillin G and streptomycin at 37°C with 5% CO<sub>2</sub>.

**Induction of Alternatively Activated RAW Macrophages by Th2 Cytokines:** The RAW264.7 cell line (1×10<sup>5</sup>) was treated with a combination of 10 ng/mL each of IL-4, IL-10, and IL-13 (Peprotech) for 72 h, with the cytokine mixture added every 24 h. The resulting cells were macrophages in alternative activation state, named as IL-treated RAW macrophages.

Analysis of Surface Molecules by Flow Cytometry: The expressions of surface molecules in RAW264.7 cells were evaluated by flow cytometry before and after treated with the combination of IL-4, IL-10, and IL-13. Briefly, the monolayers of IL-treated or the innate RAW264.7 cells were washed with cold phosphate buffer solution (PBS, pH=7.4) twice, and then were pipetted gently avoiding creating bubbles to detach the cells from the Petri dishes (Corning Co.) by the sheer force of media flowing over the cells. The cells suspension were collected and were incubated with rabbit anti-mouse monoclonal antibodies (anti-CD68 and anti-CD206; Biolegend Co.) or isotype-matched control antibodies for 1 h at 4°C in the dark. The cells were washed twice, followed by incubation with FITC-conjugated anti-rabbit antibodies for 1 h. After washing twice, the cells were analyzed by flow cytometry (Coulter EPICS XL).

Cell Proliferation Assays-MTS Assay: Both RAW and IL-treated RAW macrophages were seeded in 96-well plates at a density of  $4 \times 10^3$  cells/well and cultivated in an incubator overnight. The culture medium was replaced with 200  $\mu$ L of culture medium in which o-MWCNT was dispersed at concentrations of 0.02, 0.1, and 0.5 mg/mL. The viable cell number was determined at 24 h, 48 h, and 72 h, using the MTS assay (CellTiter 96@ Aqueous Non-Radioactive Cell Proliferation Assay, Promega) according to the manufacturer's instruction. At the end of the exposure, the culture medium containing o-MWCNT was discarded and the cells were washed twice with PBS (pH=7.4). Thereafter, 100  $\mu$ L of fresh culture medium containing 20  $\mu$ L MTS tetrazolium reagent was added to the cells. Plates were returned to the incubator for another 1.5 h at 37 °C, the culture medium was collected and the absorbance at 490 nm was recorded as OD value using a BioTek Synergy™ 4 Hybrid Multi-Mode Microplate Reader (BioTek Instruments, USA). In order to convert the OD value into viable cells number, a linear calibration curve between viable cell number and absorbance at 490 nm was founded and the viable cell number was calculated. The cell proliferation rate was calculated by the following formula: cell proliferation rate (%) = [(average cell number of sample wells) / (average cell number of control wells)]  $\times$  100. The intact culture medium was evaluated as a control. The cell morphology was also observed by inverted microscope (Olympus IX71).

Tumor Cell Migration: To measure the migration activity of 4T1 cells *in vitro*, a transwell migration assay was conducted in 24-well Millicell hanging cell culture inserts (pore size of 8  $\mu$ M, Millipore). The 4T1 cells were added to the upper chamber, and in the lower chamber were seeded (1) innate RAW macro-

phages alone or (2) incubated with o-MWCNT of 0.1 mg/mL, (3) IL-treated RAW macrophages alone or (4) incubated with o-MWCNT of 0.1 mg/mL. After 48-h incubation, the 4T1 cells on the upper surface of the filter were carefully removed by wiping with a cotton swab. The membrane was allowed to dry, and then the migrated cells were fixed with 4% paraformaldehyde and stained with 0.1% crystal violet. The crystal violet was eluted and we measured the absorbance of the eluent at a wavelength of 570 nm using a BioTek Synergy™ 4 Hybrid Multi-Mode Microplate Reader (BioTek Instruments, USA). The cell migration rate was calculated by the following formula: Relative rate of migration (%) = [absorbance with IL-treated Raw macrophages cultured in the lower chamber/absorbance with innate Raw macrophages cultured in the lower chamber]  $\times$  100. The transwell assay was carried out at least three times.

Animals and Injection Procedure: Eight-week-old, female BABL/c mice were bred at the Experimental Animal Center at the Institute of Basic Medical Sciences, Chinese Academy of Medical Sciences (Beijing, China) under specific pathogen-free conditions. All the animal experiments reported herein were carried out in compliance with the regulations of Chinese Academy of Medical Sciences Standing Committee on animal experiments. To establish the tumor-bearing mouse model, 4T1 cell suspensions in PBS (pH = 7.4) were subcutaneously inoculated into the rear backs of the naive female BALB/c mice ( $2 \times 10^6$  4T1 cells/mouse). Most of the mice developed visible solid tumors ( $\geq 4$  mm in diameter) by post-inoculation day 7. The well-established 4T1 tumor-bearing mice were randomly divided into 2 groups: control group (n = 6) and o-MWCNT group (n = 6). The o-MWCNT group was subcutaneously injected twice with o-MWCNT solution at a dose of 0.1 mg/mouse, once a week. The control group was injected with the same volume of water. One week after the second injection, three mice from each group were intravenously given ultra small paramagnetic iron oxide (Sinerem®, Laboratoire Guerbet, Aulnay sous Bois, France) at a dose of 2  $\mu$ mol/mouse. The mice were sacrificed at 24 h post Sinerem® injection. The tissues surrounding the o-MWCNT injection site, tumor tissue, and lung tissue were excised and fixed in 10% neutral buffered formalin. All materials were sterilized before being introduced into the animals.

Histological and Immunohistochemical Analysis: After conventional processing, paraffin-embedded sections of subcutis, lung, and tumor tissues were prepared as described previously [22]. To evaluate iron location, sections were stained with Perl's stain, which yields a bright blue product. In

brief, equal parts of hydrochloric acid and potassium ferrocyanide were mixed prior to use. The sections were immersed in the solution for 20 minutes, washed well in distilled water, and counterstained with neutral red for 5 minutes. The iron parts became bright blue and the nuclei parts became red. The lung tissue and tumor tissue were stained with an HE protocol. The sections of tumor tissue were also stained for CD31 antigen with a primary rabbit polyclonal antibody CD31 (Beijing Biosynthesis and Biotechnology Co., LTD China) using standard immunohistochemistry techniques. CD31 was detected with a DAB kit for peroxidase staining, and sections were counterstained with hematoxylin. The stained sections were subjected to microscopy (Leica DMI4000B).

**ICP-MS Assay:** Subcutis and tumor tissues were weighted precisely and soaked in digestion solution consisting of high purity nitric acid, sulfuric acid, and perchloric acid. They were then heated at 60°C and diluted using distilled water. Inductively coupled plasma mass spectrometry (ICP-MS, Thermo ICP-MS XII) was applied to examine the iron content in the solution and the iron concentration ( $\mu\text{g/g}$ ) in each tissue was calculated.

**Statistical Analysis:** Data are expressed as average  $\pm$  standard deviation ( $\bar{x} \pm \text{SD}$ ) unless otherwise stated. Data were analyzed using a student's

two-tailed test, assuming equal variance, with SAS 8.2 software.

## Results and Discussion

**Physicochemical Characterization of o-MWCNT:** In order to understand the chemical and physical properties of the o-MWCNT, we characterized its features in solid state as well as dispersed in water, using SEM, DLS, UV-vis-NIR spectroscopy, FTIR, XPS, and TGA. Figure 1 displays the chemical and physical characteristics of o-MWCNT dispersed in water. A representative SEM image shows that after oxidization, a-MWCNT was cut short, but the tube-like structure was well maintained. By counting the o-MWCNT in 10 randomly selected SEM images, the length distribution of o-MWCNT was estimated as ranging from 500 nm to 2  $\mu\text{m}$ , with an average length of 974 nm, as shown in the plots inserted in the SEM image. DLS data provided information about the hydrodynamic diameter of nanotubes as well as the range of size distributions (Fig. 1B). Surface chemical features of o-MWCNT were analyzed by UV-vis-NIR spectroscopy, XPS, FTIR, and TGA. Figure 1C presents characteristic absorption of o-MWCNT in 240-265 nm.

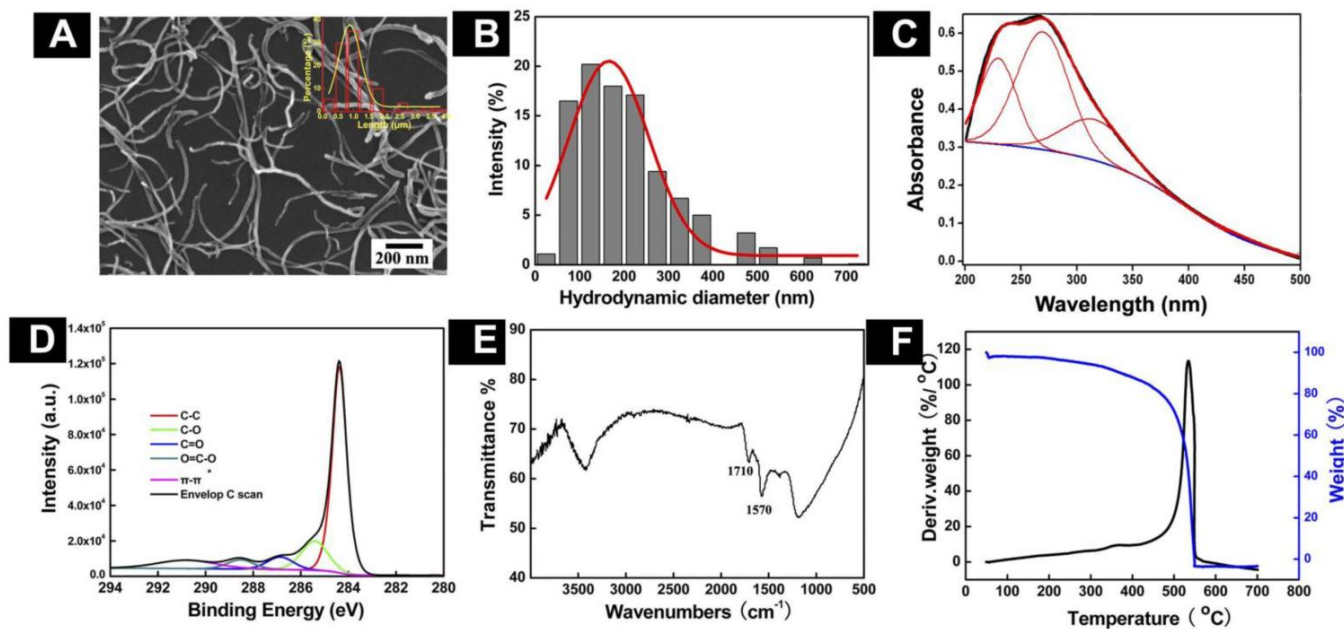


**Figure 1.** Physicochemical characterization of o-MWCNT. (A) Representative SEM image with inserted plot of size distribution. (B) Distribution of hydrodynamic diameters. (C) Absorption spectrum enveloping three resolved peaks. (D) C1s spectrum; (E) FTIR spectrum; and (F) TGA and DTG spectra.

In our previous work, we demonstrated that the spectrum could be resolved into three peaks [25], the intensity of peak 2 was well associated with the oxidation degree of o-MWCNT, and the wavelength of peak 2 varied with the size distribution of o-MWCNT. The characteristic binding energies of o-MWCNT in the C1s spectrum included 284.4 eV, 285.4 eV, 286.9 eV, 288.6 eV, and 290.8 eV (Fig. 1D), which were attributed to C-C, C-O, C=O, O-C=O, and  $\pi$ - $\pi$ , respectively, indicating that a variety of oxygen-containing groups had been introduced to the surface of o-MWCNT. FTIR spectroscopy provided further evidence of the O-C=O group existing on the surface, based on the characteristic absorption peak of 1720  $\text{cm}^{-1}$  (Fig. 1E). Results from TGA and DTG showed that the oxidation temperature of o-MWCNT was 504.4°C, which was substantially lower than the temperature of 651°C for a-MWCNT (Fig. 1F). This variation in the temperature reflected defects that resulted from surface oxidation.

The o-MWCNT Inhibited M2 Macrophage Proliferation *In Vitro*: After incubation with the combination of IL4, IL10, and IL13 for 72 h, cell expression of

CD206 was up-regulated (Supplementary Material: Fig. S1), which was consistent with previously reported results and indicated that the IL-treated RAW macrophages had processed characteristics of tumor associated macrophages [13]. Various assays have been used to examine cells viability. Angeles Jos et al. [26] had applied different assay including neutral red uptake, protein content, MTS metabolization, LDH leakage and trypan blue exclusion test to examine the effect of oxidized single walled carbon nanotubes (COOH-SWCNTs) on the viability of differentiated or non-differentiated Caco-2 cells. Their results showed that MTS metabolization assay and neutral red uptake assay were more sensitive than the others when the concentration range of COOH-SWCNTs was 0~1000  $\mu\text{g}/\text{mL}$ . In our current work, the concentration of o-MWCNT varied from 0 to 500  $\mu\text{g}/\text{mL}$ , therefore, MTS assay was employed to examine and compare the effect of o-MWCNT on the growth of innate RAW or IL-treated RAW macrophages incubated with different concentrations of o-MWCNT for 72-h (Fig. 2).

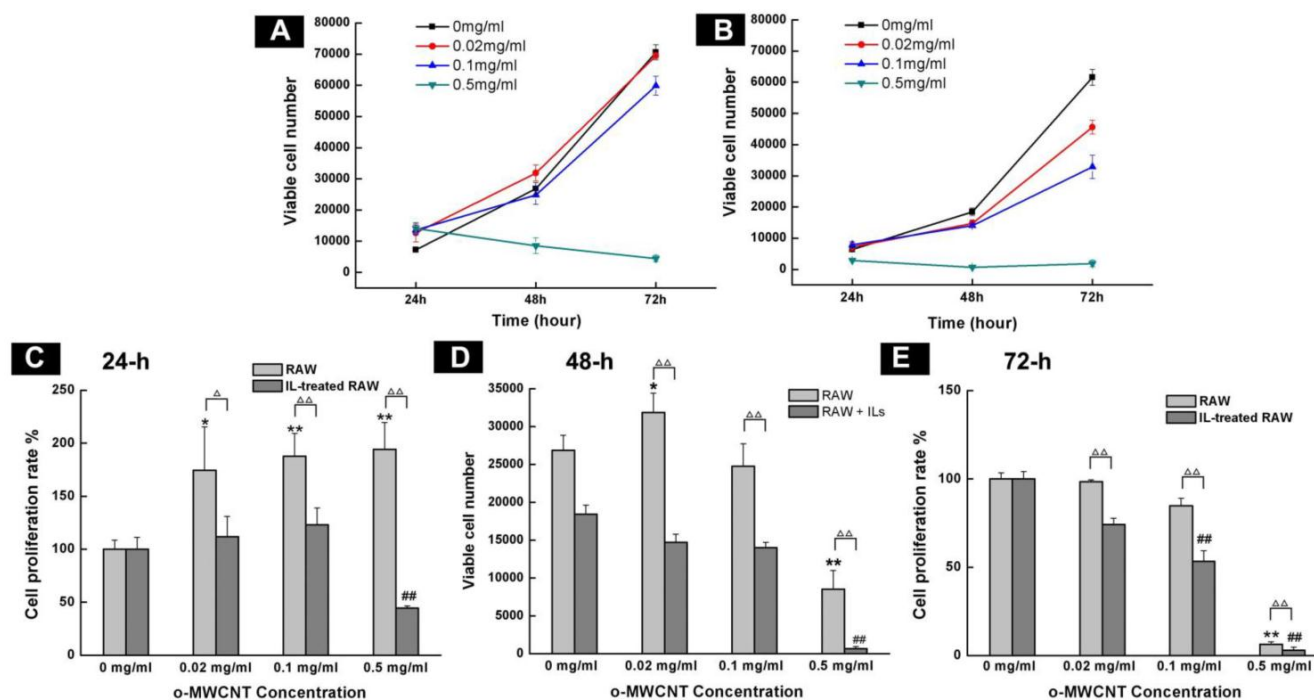


**Figure 2.** Influence of o-MWCNT on the proliferation of innate RAW and IL-treated RAW macrophages. (A-B) Viable cells number of innate RAW and IL-treated RAW macrophages after incubated with o-MWCNT at 24, 48, and 72-h. (C-E) Proliferation rate comparison between innate RAW and IL-treated RAW macrophages incubated with different concentration of o-MWCNT for 24, 48, and 72-h. \*represents significant difference from innate RAW macrophages unexposed to o-MWCNT (\*:  $p < 0.05$ , \*\*:  $p < 0.01$ ). # represents significant difference from IL-treated RAW macrophages unexposed to o-MWCNT (#:  $p < 0.05$ , ##:  $p < 0.01$ ).  $\Delta$  represents comparison between RAW and IL-treated RAW macrophages.  $n=3$ .

The starting cells number was the same for the innate RAW and IL-treated RAW. Except for at the highest concentration of 0.5 mg/mL, both innate RAW and IL-treated RAW macrophages proliferated more with prolonged incubation time, however, the viable cells number for IL-treated RAW macrophages was substantially less than that for the innate RAW macrophages at 24-h, 48-h, and 72-h of exposure to o-MWCNT with different concentrations; and the highest concentration of 0.5 mg/mL inhibited proliferation of both innate RAW and IL-treated RAW macrophages (Fig. 2A-B). The effect of o-MWCNT concentration was more complex (Fig. 2C-E). The highest concentration of 0.5 mg/mL induced the strongest inhibition of proliferation of either innate RAW or IL-treated RAW macrophages at each time point. In further comparison, within the first 24-h incubation, proliferation rate of innate RAW or IL-treated RAW macrophages was enhanced in direct correlation with the increase in o-MWCNT concentration; however, IL-treated RAW macrophages exhibited obviously lower proliferation rate compared with innate RAW macrophages. When incubation time was prolonged, proliferation rate of IL-treated RAW macrophages began to decrease with an increase in o-MWCNT concentration, while the proliferation rate of innate RAW macrophages was changed little in reference to the control. These results showed that o-MWCNT had different effect on the proliferation rate of innate RAW and IL-treated RAW macrophages. As incubation time was prolonged to 48-h, in the concentrations of 0.02 mg/mL and 0.1 mg/mL, the o-MWCNT inhibited the proliferation rate of IL-treated RAW macrophages while not affected that of innate RAW macrophages.

The morphological images of innate RAW and IL-treated RAW macrophages after exposure to different concentrations of o-MWCNT for 48-h are shown in Figure 3. The IL-treated RAW macrophages became bigger in size compared to the innate RAW macrophages. When incubated with different concentration of o-MWCNT, the IL-treated RAW macrophages exhibited reduced ability to engulf o-MWCNT compared to the innate RAW macrophages. In general the innate RAW macrophages exhibited a better growth status compared to IL-treated RAW macrophages at each exposure concentration of o-MWCNT for 48-h. It could be also noticed that no matter exposed or not to o-MWCNT, the viable cells number of IL-treated RAW became less than that of the innate RAW macrophages after 48-h incubation though they both have the same starting cells number of  $4 \times 10^3$ . This is consistent with the results obtained

from the MTS assay.

The o-MWCNT Addition into IL-Treated RAW Cells Inhibited 4T1 Tumor Cell Migration: Macrophages in the alternative activation state primarily consist of tumor-associated macrophages (TAMs), which actually promote tumor cell proliferation and metastasis [27]. Here, we investigated the migration of 4T1 breast carcinoma cells when they were co-incubated in a transwell device with innate RAW or IL-treated RAW macrophages that were exposed to o-MWCNT. The results are shown in Figure 4. The tumor cells in the upper well exhibited significantly higher migration when co-incubated with IL-treated RAW macrophages in the lower well, while significantly decreased migration was observed for the tumor cells when IL-treated RAW macrophages in the lower well were exposed to o-MWCNT at the concentration of 0.1 mg/ml for 48-h. These results indicate that o-MWCNT altered the ability of IL-treated RAW macrophages to promote tumor cell migration.

Subcutaneously Injected o-MWCNT Attracted Macrophages: In order to examine the biodistribution of macrophages in the injection subcutis tissue and in the tumor tissue, we utilized ultra small paramagnetic iron oxide (USPIO) nanoparticles as an indicator to show the variation of macrophages in the tissues. USPIO nanoparticles are one type of contrast for magnetic resonance (MR) imaging due to their cell-specificity for macrophages and usually used for magnetic resonance of lymph nodes [28]. After IV injection, USPIO nanoparticles enter the interstitial space from blood vessels and can be intracellularly trapped in tissue macrophages and visualized in tissue by Perl's blue staining. Therefore, the blue area and iron content in the tissues can indicate the distribution and amount of macrophage in the tissue. Figure 5 presented histological observations of mice subcutis received IV injection of USPIO after subcutaneous administration of o-MWCNT injection or the same volume of water for one weeks. Figure 5A and Figure 5C gave subcutis sections stained by H & E, showing that the subcutaneously injected o-MWCNT were taken up by the cells and aggregated in the subcutis. This phenomenon was also reported by our previous work that most subcutaneously injected o-MWCNT was taken up by resident macrophages around the injection site [21-22]. It is interesting to note that in Perl's blue-stained sections there were many blue-stained cells in the subcutis around the o-MWCNT aggregation (Fig. 5B), while no obvious "blue" cells could be seen in the control subcutis (Fig. 5D).

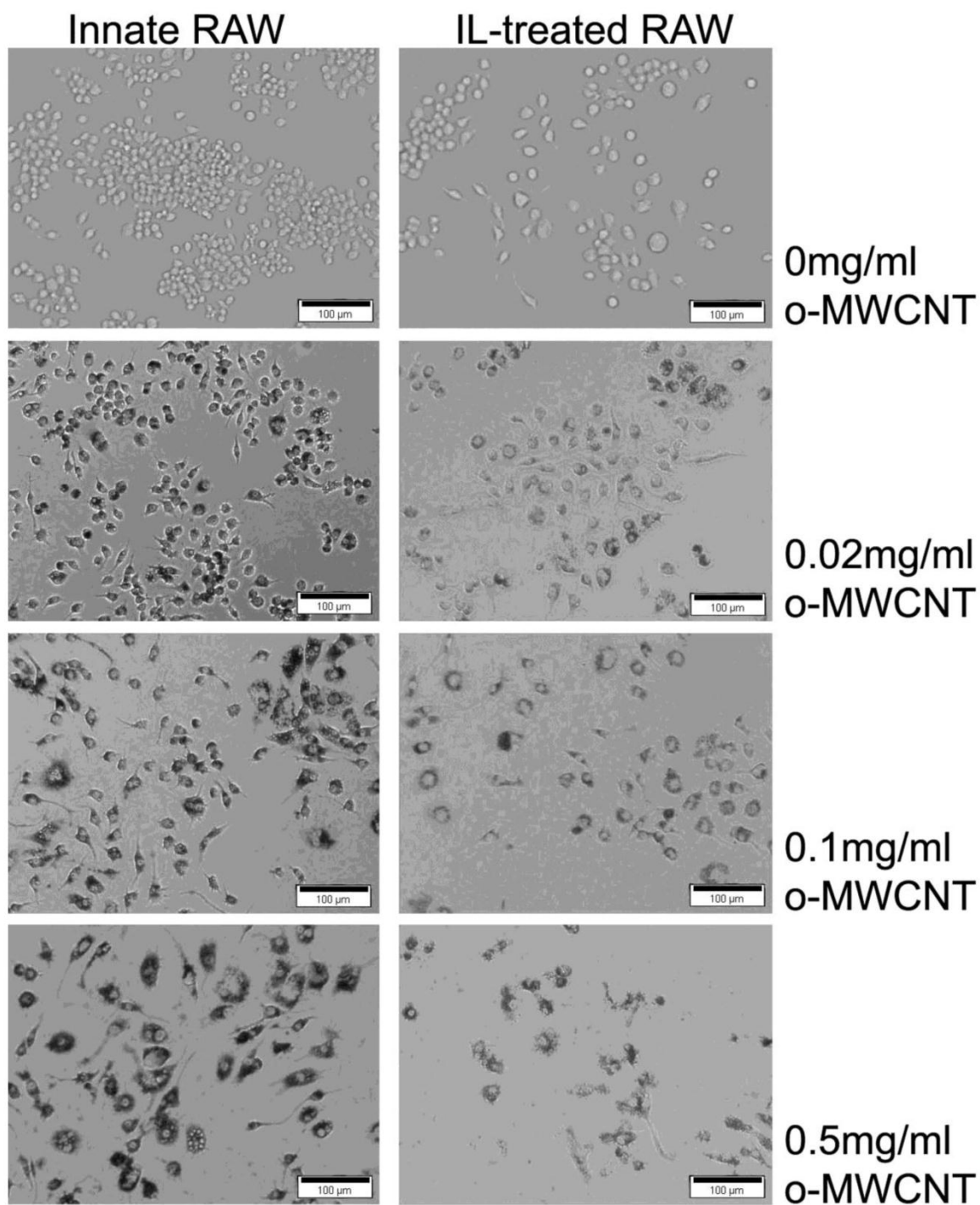


**Figure 3.** Representative optical microscopy observations of innate RAW and IL-treated RAW macrophages incubated with o-MWCNT for 48-h at different concentrations.

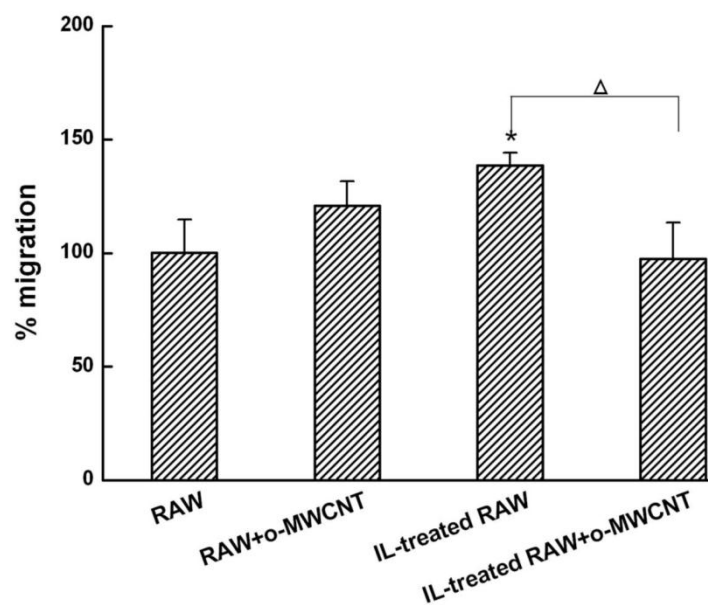


**Figure 4.** The o-MWCNT suppressed the ability of IL-treated RAW macrophages to enhance tumor cell migration. \*represents significant difference from innate RAW macrophages unexposed to o-MWCNT (\*:  $p < 0.05$ ). <sup>Δ</sup>represents significant difference between IL-treated RAW macrophages un- and exposed to o-MWCNT (<sup>Δ</sup>:  $p < 0.05$ ). n=3.

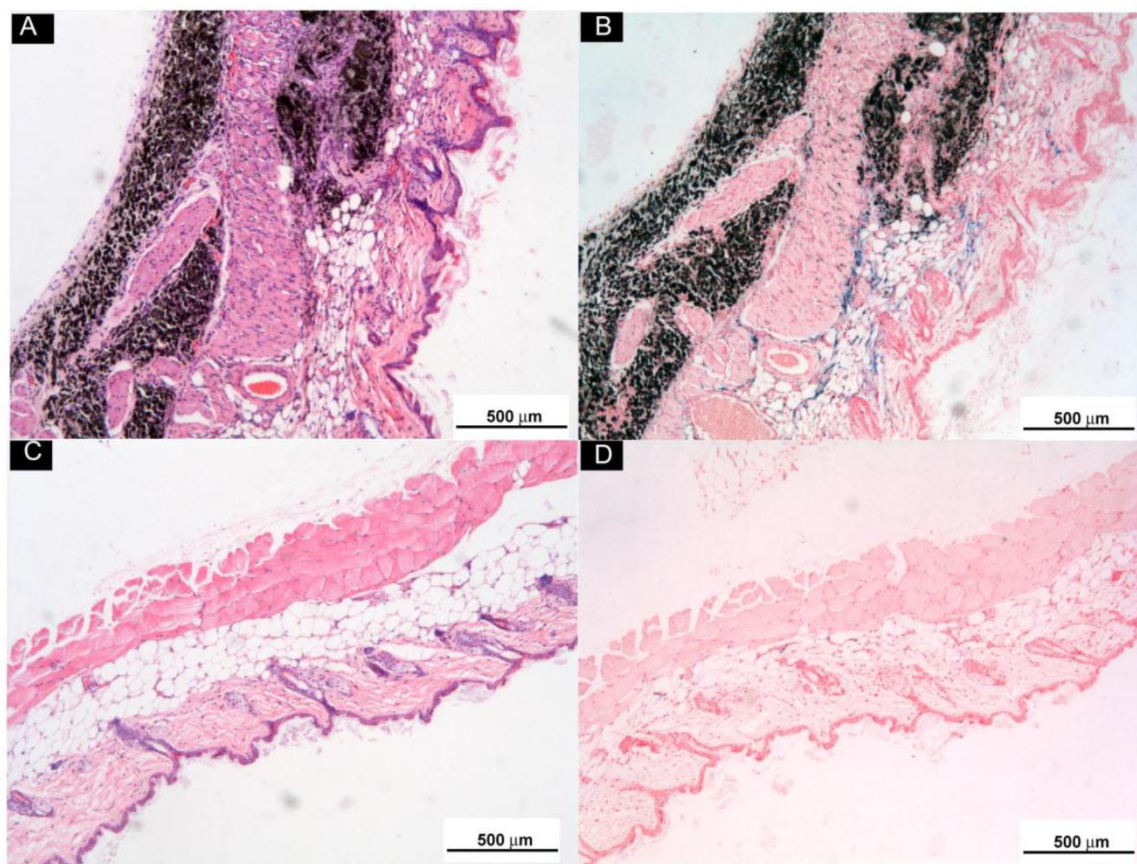


**Figure 5.** Histological observations of subcutis around subcutaneously injected o-MWCNT or water by H & E and Perl's blue-staining. (A) and (B): Subcutis tissues stained by H & E and by Perl's blue around injection site of o-MWCNT injection; (C) and (D): Subcutis tissues stained by H & E and by Perl's blue around injection site of control.

According to the characteristics of USPIO mentioned above, we considered that these blue cells were new coming macrophages attracted by the aggregated o-MWCNT from interstitial space, implying the aggregated o-MWCNT attracted macrophages constantly in the experimental period.

The o-MWCNT Reduced Macrophages in Tumor Microenvironment: Macrophages within the tumor microenvironment are referred to as tumor-associated

macrophages (TAMs) and most are derived from peripheral blood monocytes recruited into the tumor mass [29]. Here we examined whether the subcutaneously injected o-MWCNT induced variation of macrophages amount in the tumor microenvironment. Fig. 6A shows an optical image of whole tumor mass stained with Perl's blue, showing that there were bright blue areas around the tumor mass.

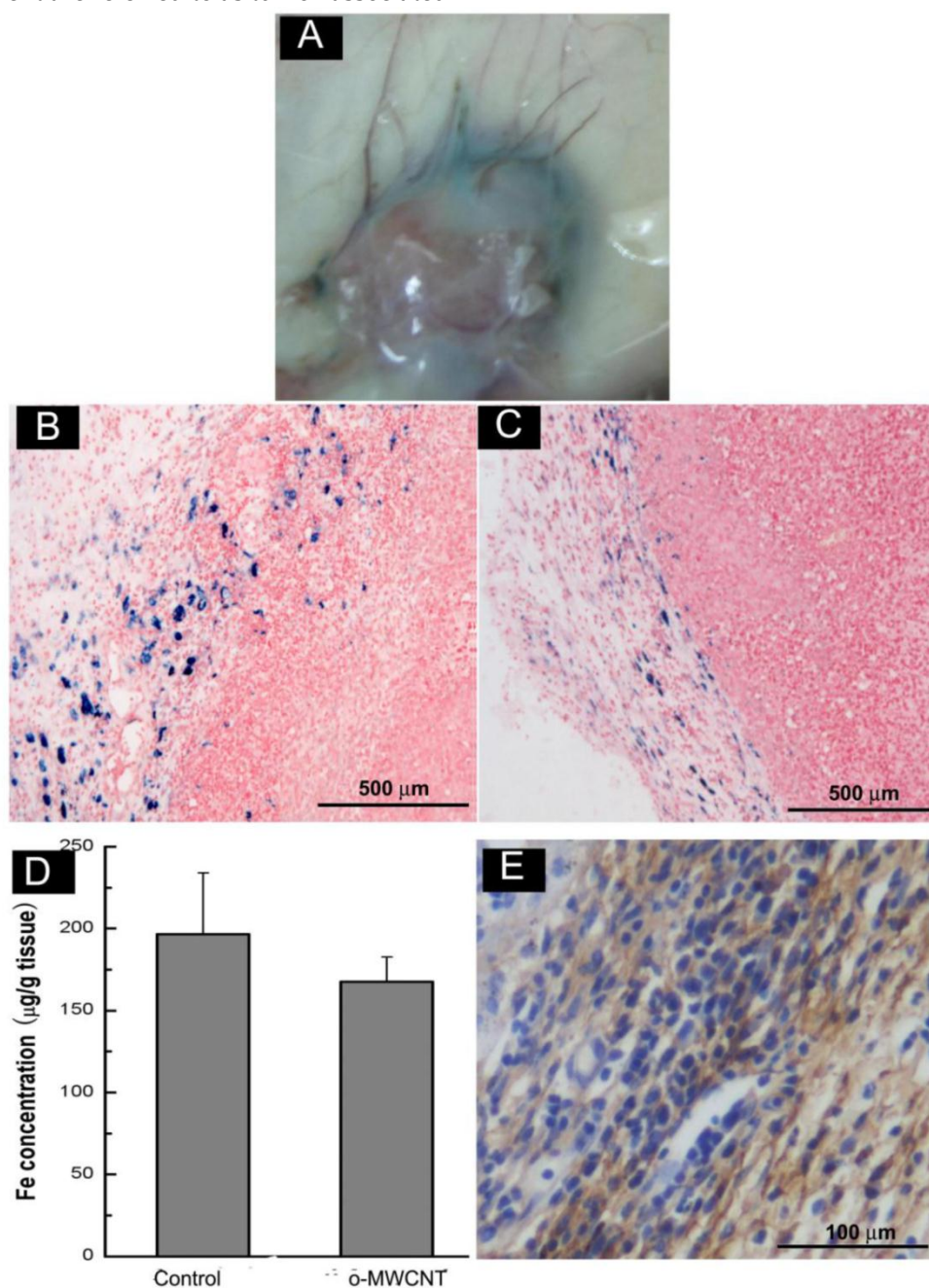


**Figure 6.** Subcutaneous injection of o-MWCNT reduced macrophages in the tumor microenvironment. (A) Anatomical morphology of tumor mass stained by Perl's blue. (B) Histological analysis of tumor tissue stained with Perl's blue of control mouse. (C) Histological analysis of tumor tissue stained with Perl's blue of o-MWCNT injection mouse. (D) ICP-MS analysis of iron concentration in tumor mass of control and o-MWCNT injection mice, (n=3). (E) Immunohistochemical staining of macrophage in the tumor tissue sections with anti-F4/80.

Further observation in Perl's blue-stained tissue sections (Fig. 6B-C) showed there were many cells in intense blue in the tumor margin. When comparing Fig. 6B and Fig. 6C, it seemed that the tumor tissue of the o-MWCNT group appeared to have less blue areas than that of the tumor control group, and this observation was proven by the result of ICP-MS analysis (Fig. 6D), showing that there was less iron of USPIO detected in the tumor mass of the o-MWCNT group. The cells in blue in the tumor margin were further identified as macrophages by F4/80 expression (Fig. 6E). As IV injected USPIO nanoparticles mostly enter the interstitial space from blood vessels and can be engulfed by macrophages, the results in Fig. 6 indicated that there were tumor associated macrophages in the tumor microenvironment, and the macrophages number in the o-MWCNT group was less than that in the control group. It is believed that macrophages within the tumor microenvironment are derived from peripheral blood monocytes recruited into the tumor, rather than from local tissue macrophages [29]. Therefore, it could be inferred that the reduction of macrophages in the tumor microenvironment was associated with the interaction of o-MWCNT to the

macrophages, which competitively attracted macrophages with the tumor, decreasing their probability of entering into the tumor mass.

**The o-MWCNT Reduced Vessels in Tumor Microenvironment:** It has been suggested that tumor cells "educate" macrophages in the tumor microenvironment to perform supportive roles that promote tumor progression, metastasis, angiogenesis, and immunosuppression [30]. The number of macrophages in the tumor microenvironment is proportionally associated with formation of neovasculature [31]. Here, we examined vessels in the tumor microenvironment by histological and immunohistochemical observation. It was showed that there were more vascular structures around the tumor mass in the control group than in the o-MWCNT group (Fig. 7A-B). This observation was proved by the results of statistically counting the vessel density in five randomly selected areas in three sections for each group (Fig. 7C). Immunohistological staining of vascular endothelium cells with anti-CD31 antibody further proved that the vessel density of the o-MWCNT group was less than that of the control group (Fig. 7D-E).

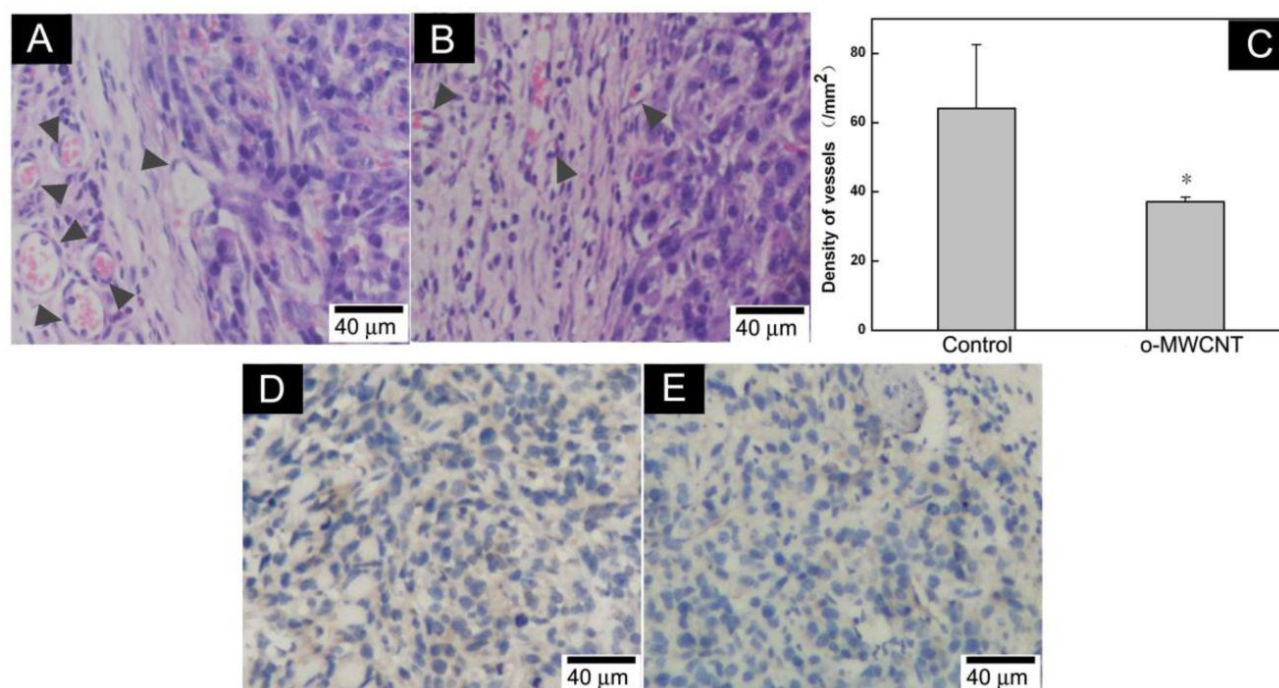


**Figure 7.** Variation of vessel density in the tumor tissues. (A) Histological analysis of vessels in HE stained tumor tissue sections of control mouse; (B) Histological analysis of vessels in HE stained tumor tissue sections of o-MWCNT injection mouse; Vascular structures indicated by dark gray arrow heads. (C) Vessel density statistically counted under microscope, \*:  $P < 0.05$ . (D) Immunohistochemical analysis of CD31 in tumor tissue of control mouse; (E) Immunohistochemical analysis of CD31 in tumor tissue of o-MWCNT injection mouse, CD31 positive structure was stained in brown color.

Fig. 8 presents the outcome of the tumor progression and lung metastasis status at termination of the experimental period. Tumor cells in the control group showed features of heavy proliferation, indicated by marked variation in the size and shape of their nuclei, with hyperchromatism and numerous mitoses (Fig. 8A and C). In contrast, tumor cells in the o-MWCNT group exhibited shrunken nuclei and a lot of pores appearing in the tumor mass (Fig. 8B and D). The 4T1 cell is highly metastatic and lung metastasis was found in the control group (Figure 8E), while no obvious metastasis was observed in the lungs of the o-MWCNT group (Figure 8F). These result suggested that subcutaneously injected o-MWCNT had an inhibitory effect on tumor lung metastasis.

Our previous investigation demonstrated that subcutaneously injected o-MWCNT upregulated the expression of GM-CSF and IL12p70 in the serum, the both obtained 2.17- fold and 2.0-fold increase [22]. The two cytokines are typical ones that are secreted by macrophages when they are activated classically and associated with anti-tumor responses. The current work provided influence of o-MWCNT upon the macrophages from another aspect. Taken together, our investigation demonstrated that the o-MWCNT not only activated the macrophages in classical way to elicit antitumor responses, but also recruited macrophages to reduce macrophages in the tumor micro-environment, which is benefit to altering tumor microenvironment and modifying tumor progression.

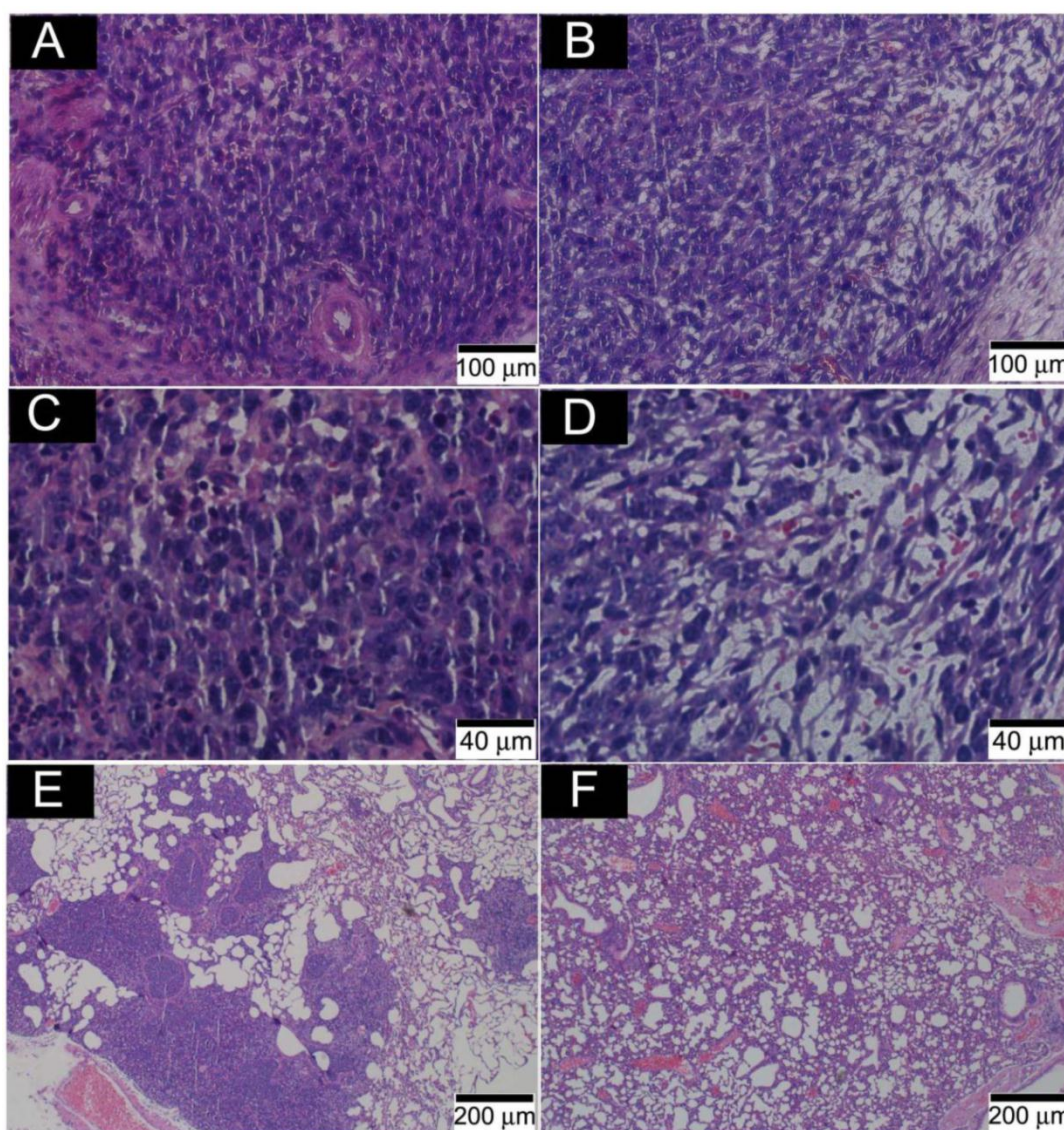


**Figure 8.** Histological analysis of tumor and lung metastasis in the control and o-MWCNT injection mice. (A) and (C): Histological observation of tumor tissues of control group. (B) and (D): Histological observation of tumor tissues of o-MWCNT injection group. (E): Lung metastasis of control group. (F): Lung metastasis of o-MWCNT injection mice.

## Conclusion

Subcutaneous injection of o-MWCNT in the tumor-bearing mice not only attracted resident macrophages around the injection site and induced phagocytosis, but also competed with the tumor mass for recruitment of macrophages from circulating monocytes. These interactions led to macrophages reduction and decreased vessel density around the tumor mass, which contributed to the inhibition of tumor progression and metastasis in the lung. For the IL-treated RAW macrophages, o-MWCNT suppressed their ability to promote tumor cell migration, as well as decreased their proliferation rate.

## Acknowledgement

Authors thank for financial support from National Key Program of China (973 program 2011CB933504 and 2010CB934002), National Natural Science Foundation of China (NSFC 81000665) and Beijing Municipal Natural Science Foundation (7092063).

## Supplementary Material

Fig. S1. <http://www.thno.org/v02p0258s1.pdf>

## Conflict of Interest

The authors have declared that no conflict of interest exists.

## References

- Mukhtar RA, Nseyo O, Campbell MJ, Esserman LJ. Tumor-associated macrophages in breast cancer as potential biomarkers for new treatments and diagnostics. *Expert Rev Mol Diagn.* 2011; 11(1): 91-100.
- Mosser DM, Edwards JP. Exploring the full spectrum of macrophage activation. *Nat Rev Immunol.* 2008; 8(12): 958-69.
- Pollard JW. Tumour-educated macrophages promote tumour progression and metastasis. *Nat Rev Cancer.* 2004; 4(1): 71-8.
- Yu JL, Rak JW. Host microenvironment in breast cancer development: inflammatory and immune cells in tumour angiogenesis and arteriogenesis. *Breast Cancer Res.* 2003; 5(2): 83-8.
- Luo YP, Zhou H, Krueger J, Kaplan C, Liao D, Markowitz D, Liu C, Chen T, Chuang TH, Xiang R, Reisfeld RA. Knockdown of Fra-1 in RAW macrophages by siRNA downregulates IL-6 and Stat3, decreases the release of pro-angiogenesis factors and inhibits migration and invasion of 4T1 breast cancer cells. *Oncogene.* 2010; 29(5):662-73.
- Josson S, Matsuoka Y, Chung LW, Zhou HE, Wang R. Tumor-stroma coevolution in prostate cancer progression and metastasis. *Semin Cell Dev Biol.* 2010; 21(1): 26-32.
- Watters JJ, Schartner JM, Badie B. Microglia function in brain tumors. *J Neurosci Res.* 2005; 81(3): 447-55.
- Aldinucci D, Gloghini A, Pinto A, De Filippi R, Carbone A. The classical Hodgkin's lymphoma microenvironment and its role in promoting tumour growth and immune escape. *J Pathol.* 2010; 221(3): 248-63.
- Takayama H, Nishimura K, Tsujimura A, Nakai Y, Nakayama M, Aozasa K, Okuyama A, Nonomura N. Increased infiltration of tumor associated macrophages is associated with poor prognosis of bladder carcinoma in situ after intravesical bacillus Calmette-Guerin instillation. *J Urol.* 2009; 181(4): 1894-900.
- Wang R, Zhang J, Chen S, Lu M, Luo X, Yao S, Liu S, Qin Y, Chen H. Tumor-associated macrophages provide a suitable microenvironment for non-small lung cancer invasion and progression. *Lung Cancer.* 2011; 74(2): 188-96.
- Utrera-Barillas D, Castro-Manrreza M, Castellanos E, Gutiérrez-Rodríguez M, Arciniega-Ruiz de Esparza O, García-Cebada J, Velazquez JR, Flores-Reséndiz D, Hernández-Hernández D, Benítez-Bribiesca L. The role of macrophages and mast cells in lymphangiogenesis and angiogenesis in cervical carcinogenesis. *Exp Mol Pathol.* 2010; 89(2): 190-6.
- Hussein MR. Tumour-associated macrophages and melanoma tumorigenesis: integrating the complexity. *Int J Exp Pathol.* 2006; 87(3): 163-76.
- Luo Y, Zhou H, Krueger J, Kaplan C, Lee SH, Dolman C, Markowitz D, Wu W, Liu C, Reisfeld RA, Xiang R. Targeting tumor-associated macrophages as a novel strategy against breast cancer. *J Clin Invest.* 2006; 116(8): 2132-41.
- Sahoo NG, Bao H, Pan Y, Pal M, Kakran M, Cheng HK, Li L, Tan LP. Functionalized carbon nanomaterials as nanocarriers for loading and delivery of a poorly water-soluble anticancer drug: a comparative study. *Chem Commun (Camb).* 2011; 47(18): 5235-7.
- Tan A, Yildirim L, Rajadas J, De La Peña H, Pastorin G, Seifalian A. Quantum dots and carbon nanotubes in oncology: a review on emerging theranostic applications in nanomedicine. *Nanomedicine (Lond).* 2011; 6(6): 1101-14.
- Posadas I, Guerra FJ, Ceña V. Nonviral vectors for the delivery of small interfering RNAs to the CNS. *Nanomedicine (Lond).* 2010; 5(8):1219-36.
- Cheung W, Pontoriero F, Taratula O, Chen AM, He H. DNA and carbon nanotubes as medicine. *Adv Drug Deliv Rev.* 2010; 62(6): 633-49.
- Al-Jamal KT, Gherardini L, Bardi G, Nunes A, Guo C, Bussy C, Herrero MA, Bianco A, Prato M, Kostarelos K, Pizzorusso T. Functional motor recovery from brain ischemic insult by carbon nanotube-mediated siRNA silencing. *Proc Natl Acad Sci.* 2011; 108(27): 10952-57.
- Ladeira MS, Andrade VA, Gomes ER, Aguiar CJ, Moraes ER, Soares JS, Silva EE, Lacerda RG, Ladeira LO, Jorio A, Lima P, Leite MF, Resende RR, Guatimosim S. Highly efficient siRNA delivery system into human and murine cells using single-wall carbon nanotubes. *Nanotechnology.* 2010; 21(38): 385101.
- Huang P, Xu C, Lin J, Wang C, Wang X, Zhang C, Zhou X, Guo S, Cui D. Folic acid-conjugated graphene oxide loaded with photosensitizers for targeting photodynamic therapy. *Theranostics.* 2011; 1: 240-50.
- Meng J, Yang M, Jia F, Xu Z, Kong H, Xu H. Immune responses of BALB/c mice to subcutaneously injected multi-walled carbon nanotubes. *Nanotoxicology.* 2010; 5(4): 583-91
- Meng J, Yang M, Jia F, Kong H, Zhang W, Wang C, Xing J, Xie S, Xu H. Subcutaneous injection of water-soluble multi-walled carbon nanotubes in tumor-bearing mice boosts the host immune activity. *Nanotechnology.* 2010; 21(14): 145104.
- Meng J, Meng J, Duan J, Kong H, Li L, Wang C, Xie S, Chen S, Gu N, Xu H, Yang XD. Carbon nanotubes conjugated to tumor lysate protein enhance the efficacy of an antitumor immunotherapy. *Small.* 2008; 4(9): 1364-70.
- Jia F, Wu L, Meng J, Yang M, Kong H, Liu T and Xu H. Preparation, characterization and fluorescent imaging of multi-walled carbon nanotube- porphyrin conjugate. *Journal of Materials Chemistry,* 2009; 19(47): 8950-7.
- Cheng X, Zhong J, Meng J, Yang M, Jia F, Xu Z, Kong H, Xu H. Characterization of Multiwalled Carbon Nanotubes Dispersing

- in Water and Association with Biological Effects. *Journal of Nanomaterials*. 2011; doi:10.1155/2011/938491.
26. Jos A, Pchardo S, Puerto M, Sanchez E, Grilo A, Camean AM. Cytotoxicity of carboxylic acid functionalized single wall carbon nanotubes on the human intestinal cell line Caco-2. *Toxicology in Vitro*. 2009; 23: 1491-96.
  27. Mantovani A, Sozzani S, Locati M, Schioppa T, Saccani A, Allavena P, Sica A. Infiltration of tumors by macrophages and dendritic cells: tumor-associated macrophages as a paradigm for polarized M2 mononuclear phagocytes. *Novartis Found Symp*. 2004; 256:137-45.
  28. Neuwelt EA, Várallyay P, Bagó AG, Muldoon LL, Nesbit G, Nixon R. Imaging of iron oxide nanoparticles by MR and light microscopy in patients with malignant brain tumours. *Neuro-pathol Appl Neurobiol*. 2004; 30(5): 456-71.
  29. Shih JY, Yuan A, Chen JJ, Yang PC. Tumor-Associated Macrophage: Its Role in Cancer Invasion and Metastasis. *J. Cancer Mol*. 2006; 2(3): 101-6.
  30. Pollard JW. Tumour-educated macrophages promote tumour progression and metastasis. *Nat Rev Cancer*. 2004; 4(1): 71-8.
  31. Chen JJ, Lin YC, Yao PL, Yuan A, Chen HY, Shun CT, Tsai MF, Chen CH, Yang PC. Tumor-associated macrophages: the double-edged sword in cancer progression. *J Clin Oncol*. 2005; 23(5): 953-64.